

Brewing sustainability and strength: Biocomposite development through tea waste incorporation in polylactic acid

Javad Khodadad Hatkeposhti¹, Naser Kordani¹ ,
Mohammad Akbarzadeh Pasha² and Mahdi Bodaghi³ 

Proc IMechE Part L:
J Materials: Design and Applications

1–11

© IMechE 2023



Article reuse guidelines:

sagepub.com/journals-permissions

DOI: 10.1177/14644207231221244

journals.sagepub.com/home/pil



Abstract

This study aims to enhance the mechanical properties of polylactic acid by incorporating black tea waste as an economical and sustainable additive capable of being recycled. The black tea waste, after the hot water color removal process, is milled to a fine and uniform powder size. The combination of these particles with polylactic acid is carried out using a twin-screw extruder. Specimens of pure polylactic acid and biocomposites containing 3 and 5 wt% black tea waste are manufactured using a hot press machine at a temperature of 200 °C. The filaments are also successfully extruded for three-dimensional printing purposes. Scanning electron microscopy images reveal that in the polylactic acid–3% tea biocomposite, the tea particles are appropriately dispersed within the polylactic acid matrix. The tensile test results indicate that biocomposite polylactic acid–3% tea has the highest mechanical properties, with a tensile strength of 67 MPa, demonstrating a 34% increase compared to polylactic acid. Furthermore, the biocomposite of polylactic acid–3% tea waste exhibits the best performance with a fracture energy of 2.5 kJ/m² in the impact test. Hence, polylactic acid–3% tea biocomposite can be recommended as a suitable sustainable substitute. Finally, numerical simulations are performed on biocomposites containing double keyhole notches. This analysis is conducted to observe the behavior of biocomposite models with double keyhole notch under mixed-mode loading. The critical fracture load of the models is calculated using the strain energy density criterion. It is observed that an increase in the notch inclination angle and notch radius leads to a decrease in the fracture load in the models.

Keywords

Polylactic acid, tea waste, biocomposite, sustainable composites, double keyhole notch, strain energy density, 3D printing

Date received: 12 August 2023; accepted: 2 December 2023

Introduction

Many polymers are used in the manufacturing process of components due to their ease of processing and low associated costs. As a result, extensive research is being conducted in this field.^{1,2} In this regard, composites have become one of the most widely used materials in various industries due to their diverse properties such as low weight, strength, hardness, impact resistance, and corrosion resistance.^{3–7}

The production of components using conventional methods, such as hot pressing machines, is widely used due to its high production speed for low quantities of parts and cost-effectiveness. The effects of carbon black (CB) on the mechanical properties of polylactic acid-CB (PLA-CB) biocomposite produced by hot pressing were investigated. The results showed that adding an appropriate amount of CB improves the mechanical properties of polylactic acid (PLA). However, the excessive addition of CB decreases the mechanical properties of PLA-CB

composites.⁸ Dang Feng et al. fabricated biodegradable composites of PLA and bamboo charcoal through the process of melt blending and hot pressing.⁹ The influence of incorporating this additive on the mechanical properties of the composites was examined. The morphological features of the composites were analyzed using scanning electron microscopy (SEM). The findings indicated that the addition of 40% by weight of bamboo charcoal resulted in a 2.24% enhancement in the mechanical

¹Department of Mechanical Engineering, University of Mazandaran, Babolsar, Iran

²Department of Solid State Physics, Faculty of Basic Sciences, University of Mazandaran, Babolsar, Iran

³Department of Engineering, School of Science and Technology, Nottingham Trent University, Nottingham, UK

Corresponding author:

Mahdi Bodaghi, Department of Engineering, School of Science and Technology, Nottingham Trent University, Nottingham NG11 8NS, UK.
Email: mahdi.bodaghi@ntu.ac.uk

strength compared to PLA. Avci et al.¹⁰ investigated the effects of ulexite and boron compounds on the mechanical and thermal properties of flax–PLA biocomposites. The test data indicated a significant reduction in the burning rate of up to 80%. However, the mechanical properties were adversely affected by the boron compounds, resulting in a decrease of up to 20%. Despite the decline in mechanical properties, these biocomposites were considered highly desirable for application in the automotive industry based on the results obtained.

Fused deposition modelling (FDM) is a three-dimensional (3D) printing process that uses filaments made of polymers or polymer composites as raw materials. Therefore, producing filaments with suitable properties for the FDM process is of considerable importance. Jayswal et al.¹¹ produced composite filaments of PLA, thermoplastic polyurethane (TPU), and poly(ethylene) glycol (PEG) in various ratios using a twin-screw extruder. The mechanical properties of the fibers were determined through uniaxial tensile testing. By adding PEG to the PLA-TPU blend, it was observed that the yield strength and Young's modulus of the composite filaments decreased significantly compared to the pure PLA filaments. Furthermore, it was observed that there was no significant difference in the ultimate tensile strength, but the elongation at break grew by > 500%.

The design and fabrication of composite materials, along with the prediction of their longevity, have gained significant importance due to their effectiveness in diverse industries such as automotive,¹² aerospace,^{13,14} and missile manufacturing.¹⁵ The initiation and propagation of cracks are among the most significant factors that cause the degradation of composite materials. In other words, the presence of cracks is one of the critical factors in the analysis and design of components and structures. Given the existence of cracks in numerous components and structures produced by human intervention, the field of fracture mechanics is applied to examine and analyze these types of components.^{16,17} In addition, due to the essential role of notches in the design of engineering structures, they are inevitably present in various engineering components. The presence of notch results in stress concentration and enhances the susceptibility to component failure. Therefore, it is necessary to examine the fracture behavior of notched components.^{18–20}

The present study employs the criterion of strain energy density (SED), which was first introduced by Lazzarin and Zambardi²¹ for sharp V-notch. Lazzarin and Berto²² further developed this criterion for V-notch curves. The criterion of SED, as implied by its name, is founded on the concept of energy. Its magnitude is determined within the volume or surface of a structural element and varies depending on the material composition.^{23,24} The simulation and analysis of crack propagation play a crucial role in enhancing the performance and longevity of vital components. Hence, the current study aims to examine the behavior of a double keyhole notch in a PLA composite incorporating tea waste. Sih²⁵ is

acknowledged as the pioneer of the strain energy density criterion, having introduced the assessment of the impact of SED on predicting the paths of crack propagation in brittle materials. Yishu²⁶ building upon Sih's research, conducted an analysis of crack growth under mixed mode (I + II) loading. His interpretation indicated that the theory of SED could be applied not only to brittle materials but also to materials with limited plastic zones. Soltaninezhad et al.²⁷ derived novel insights by utilizing experimental data obtained from double keyhole notch specimens made of polyethylene (HDPE-PE100) with different notch inclination angles and notch radii. To analyze the behavior of notches, they utilized mixed mode (I + II) loading conditions. They determined the critical fracture loads by combining the equivalent material concept (EMC) and SED within a specified control volume near the notch tip.

The objective of this study is to enhance the mechanical properties of PLA by incorporating tea waste as an economical, sustainable, and recyclable additive. Tensile and impact test specimens were fabricated from PLA and biocomposites containing 3% and 5% tea waste in PLA using the hot-pressing process. The filaments were also successfully produced using a desktop extruder for the purpose of 3D printing. The results indicated an increase in mechanical properties in the 3% tea waste biocomposite sample. However, an increase beyond this additive content led to a decline in mechanical properties. Consequently, the PLA–3% tea biocomposite serves as a suitable sustainable substitute for pure PLA in industries where mechanical properties hold significant importance.

Given that numerous industrial parts are susceptible to having notches or experiencing fractures, with one such geometric configuration being sampled featuring double keyhole notches, computational simulation is also performed subsequently. The aim is to employ the SED criterion for appraising the threshold load at which critical fracture load occurs in biocomposite samples featuring double keyhole notches. This evaluation covers a range of notch angles and radii, enabling an examination of the distinct conditions relevant to these particular types of notched biocomposite specimens. It was observed that as the notch inclination angle and the radius of the notch decreased, the critical failure load increased proportionally.

Materials and methods

Materials

The materials used in the present study include tea waste and PLA granules from Xtrusion Company. In this study, commercial black tea waste was used without any additives. The black tea waste underwent a three-stage process of color removal using boiling water. After thorough drying, the black tea waste was milled for 5 min to achieve a completely powdered and homogenous form, obtaining the necessary black tea waste additive for the research.

Preparation of specimens

Specimens were produced at the Polymer and Petrochemical Research Institute of Tehran. The drying process of the PLA granules involved placing them in an oven at a temperature of 80 °C for a duration of 3 to 4 h. Accurate measurements of composite percentages were conducted using a digital balance (model I-EK, AND, Japan). The biocomposite consisted of 3 and 5 wt % black tea waste, combined with 97 and 95 wt% PLA, respectively. Subsequently, the mixture of black tea waste particles and PLA underwent processing using a co-rotating twin-screw extruder (model ZSK25) manufactured by Copren in Germany in 2002. The composition parameters of the materials in the extruder are presented in Table 1.

Following that, the PLA-tea biocomposite strands produced from the extruder were crushed using the Peletizer 750 Guanulierung pelletizer machine to obtain filaments that are appropriate for 3D printers. Additionally, these crushed strands were utilized to create test specimens for conducting tensile and impact tests. To produce the specimens, their moulds were prepared using a hot-plate press process. After mold fabrication, a moisture removal and drying operation was carried out for 3 to 4 h in an oven

at a temperature of 80 °C to minimize the presence of bubbles during specimen formation. The hot-plate press machine used for this purpose was the Minitestpress model from Toyoseiki, a Japanese company, available at the Polymer and Petrochemical Research Institute in Iran. Specimens were prepared according to the ISO527-2 standard for tensile testing and the ASTM D256-Type10 standard for impact testing. This was conducted at a temperature of 200 °C during 10 min. Following this, the specimens were cooled using a manual cold press at room temperature for 5 min to facilitate the production of the desired specimens. Figure 1 depicts the process of specimen fabrication.

To produce suitable filament for 3D printing, a tabletop extruder was used, and the filament stretching process was mechanized using a conveyor belt system at an appropriate speed. The biocomposite PLA-tea was produced. Table 2 provides the parameters of the desktop extruder, and Figure 2 illustrates the PLA-3% tea filament.

Equations and simulations based on the theory of SED

In this study, double keyhole notch specimens were subjected to numerical simulations to compare their critical

Table 1. Composition parameters of materials in the extruder.

Pressure	Rotator Speed	Zone 1	Zone 2	Zone 3	Zone 4	Zone 5	Zone 6
110 bar	200 rev/min	160 °C	165 °C	170 °C	175 °C	175 °C	170 °C

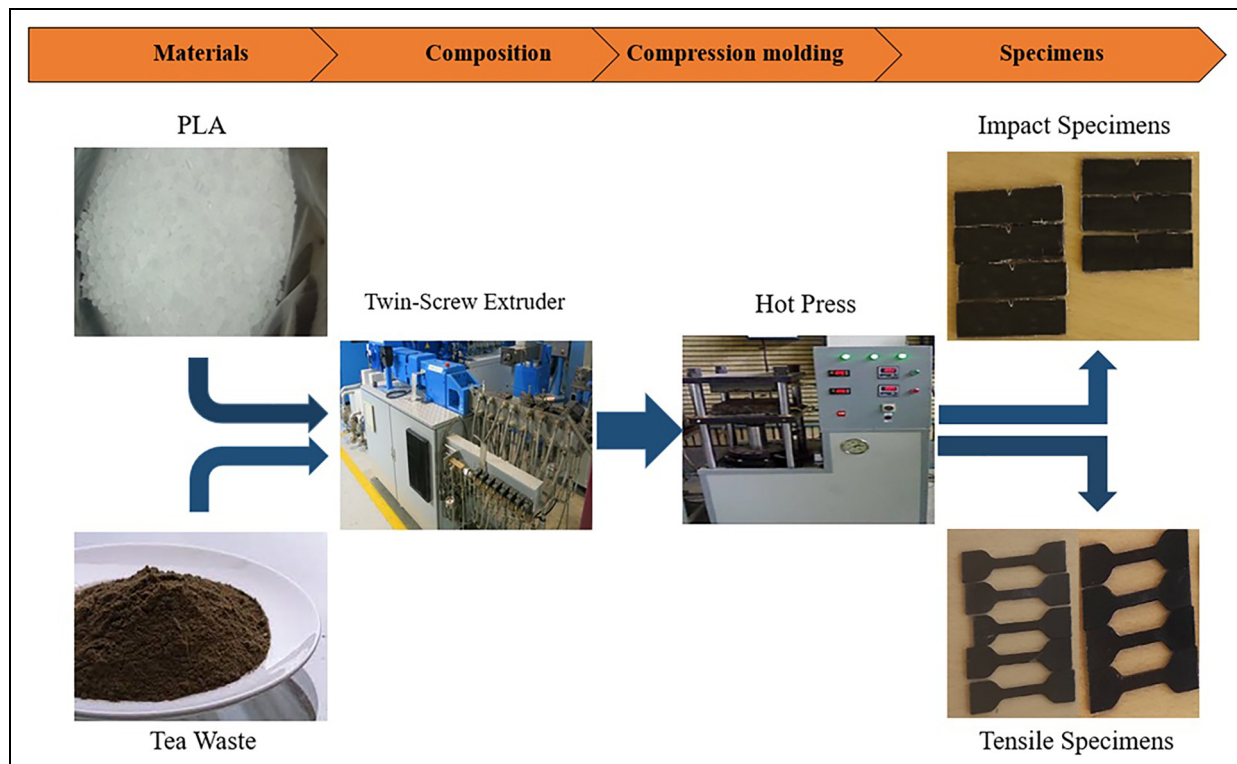


Figure 1. Process of specimen fabrication.

fracture forces in numerical modeling. Initially, the desired models were designed according to Figure 3 with three different notch radii of 0.5, 1, and 2 mm, as well as three notch inclination angles of 45°, 60°, and 75° in the software. The width of the notches was set to 1 mm.

In Figure 3, H , W , and t represent the length, width, and thickness of the specimen, respectively. The symbol “ a ” represents the distance between the centers of the two circular holes. This simulation was conducted based on the theory of SED.

Based on this theory, fracture occurs when the average strain energy density (W_{avg}) in a specified control volume to a notch reaches its critical value. The critical strain energy density (W_{cr}) is determined using the mechanical properties of the material, according to equation (1).^{21,22}

$$W_{cr} = \frac{\sigma_{ut}^2}{2E} \quad (1)$$

In equation (1), σ_{ut} and E represent the ultimate tensile strength and elastic modulus of the material, respectively. In two-dimensional investigations, the control volume neighboring the notch is defined as either a complete circle or a segment of a circle with a radius of R_c . The size of the volume surface is depicted in Figure 4 for V-notches characterized by both sharp and rounded tips.

According to Figure 4(c), the control volume for specimens with a double keyhole notch under Mode I loading is located relative to the horizontal midpoint of the notch. Under mixed mode (I + II), the control volume is no longer located in the center of the notch, but rather at a position where the principal stress reaches its maximum value next to the edge of the notch.²⁸ In the second step, the radius of the control volume circle (R_c) is

Table 2. Tabletop extruder data.

Nozzle diameter	Nozzle temperature
2 mm	190 °C

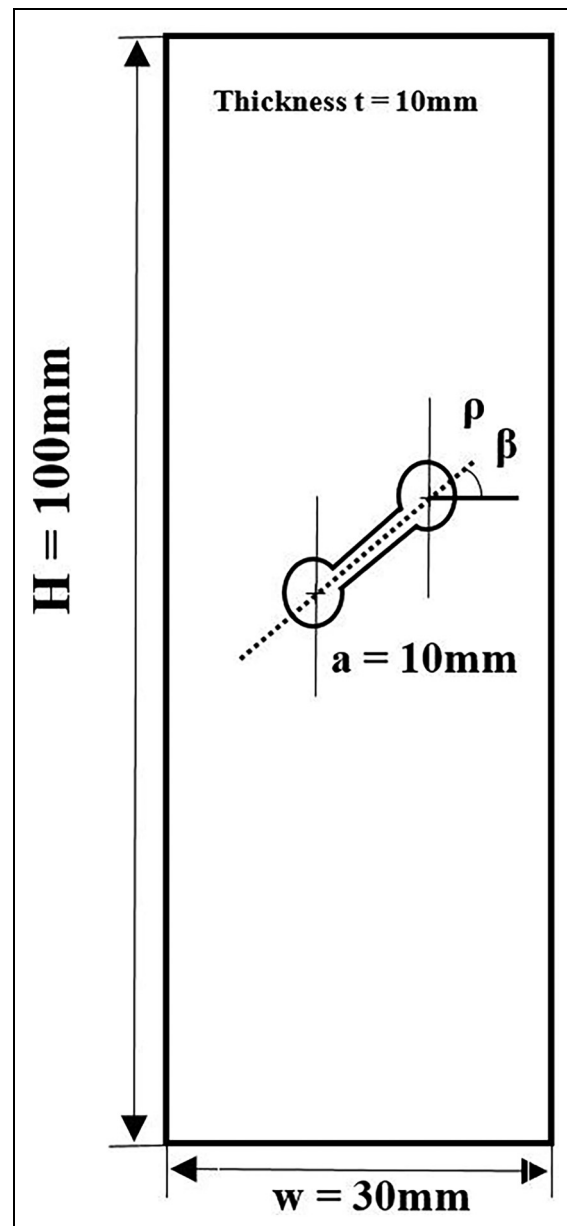


Figure 3. The geometries of the double keyhole notch models.

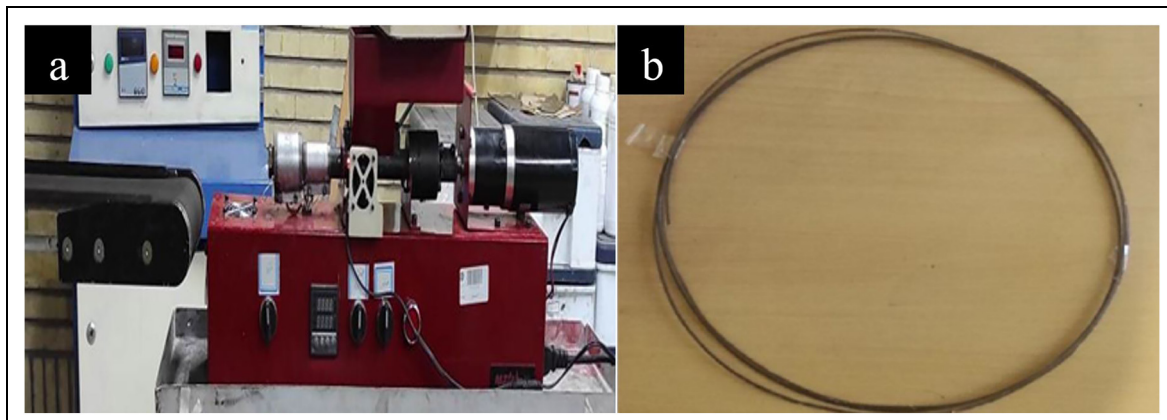


Figure 2. (a) Tabletop extruder and (b) polylactic acid (PLA)-3% tea biocomposite filament.

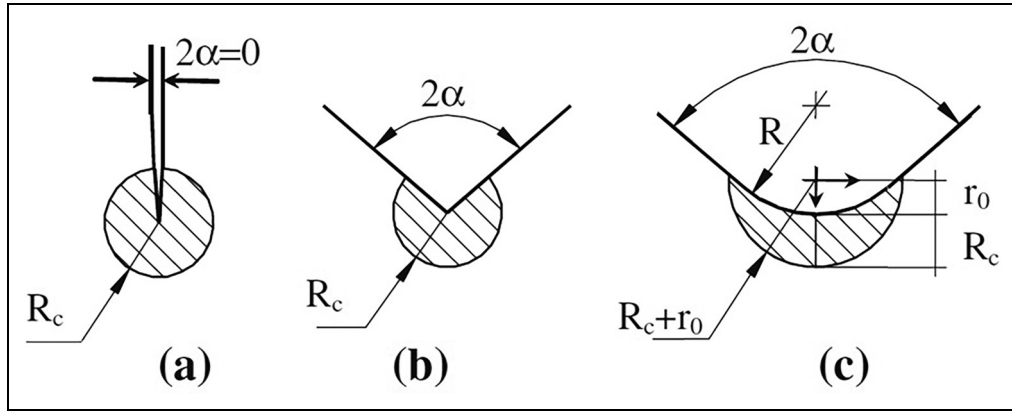


Figure 4. Critical volume definition for crack: (a) sharp V-notch, (b) blunt V-notch, and (c) rounded tips-notch.

determined by equation (2), which is a function of the ultimate tensile strength, critical fracture toughness (K_{Ic}), and Poisson's ratio (ν).²⁹

$$R_c = \frac{(1 + \nu)(5 - 8\nu)}{4\pi} \left[\frac{K_{Ic}}{\sigma_{ut}} \right]^2 \quad (2)$$

K_{Ic} represents the resistance to crack propagation when a notch is subjected to plane strain conditions and under Mode I loading. The value of K_{Ic} is dependent on the geometric dimensions of the notched body. Equation (3) uses K_{Ic} for calculation. In this equation, λ_1 represents the Williams' parameter, which is a constant equal to 0.501.³⁰ Additionally, σ_θ denotes the stress in the Y -axis direction. The value of σ_θ can be determined at various r sizes using the Abaqus software.³⁰

$$K_{Ic} = \sqrt{2\pi} \lim_{r \rightarrow 0} r^{1-\lambda_1} [\sigma_\theta(r \cdot \theta)] \quad (3)$$

The control volume circle, as depicted in Figure 5(a), moves outward from its center to a distance equal to half the radius of the notch. It should be noted that in the mixed mode state, the radius of the control surface does not change. However, its location, as shown in Figure 5(b), rotates in the direction of the maximum principal stress.³¹

In this study, simulations were conducted using the finite element analysis software ABAQUS® to obtain the W_{avg} value. Since the specimens are subjected to mixed loading conditions, it is necessary to identify the location of the maximum principal stress on the boundary of the notch first. In the initial step, the stress contour is obtained from the specimens at the boundary of the double keyhole notch. By considering the location of the maximum principal stress, the control volume rotation angle (ϕ) is determined. The precise location of the maximum principal stress is determined by capturing an image of the stress contour from ABAQUS® software and utilizing SOLIDWORKS® software's Sketch tools. The control surface is created according to Figure 6.

By applying a software load of 100 N, the simulation was performed to determine the values of strain energy (ELSE) and volume value (EVOL) on the control

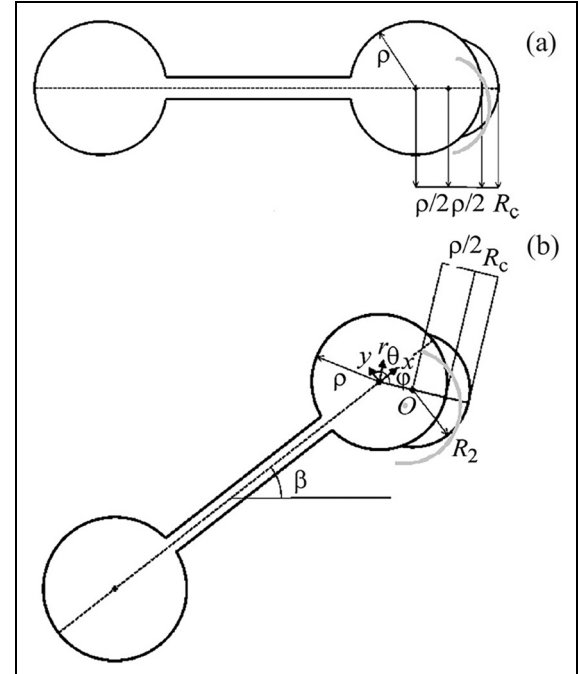


Figure 5. The control volumes in the keyhole notched specimens under (a) mode I and (b) mixed-mode conditions.

volume. The W_{avg} is determined by dividing the value of ELSE by EVOL, as stated by equation (4). The density of strain energy can be observed at the specified control volume level in Figure 7.

$$W_{avg} = \frac{ELSE}{EVOL} \quad (4)$$

Finally, according to equation (5), the critical fracture load (F_{cr}) can be determined based on the values of W_{cr} and W_{avg} .³¹

$$\frac{F_{ap}}{F_{cr}} = \sqrt{\frac{W_{avg}}{W_{cr}}} \quad (5)$$

In the above equation, the software value of load (F_{ap}), whose size is arbitrary, F_{ap} 100 N is entered into the software.

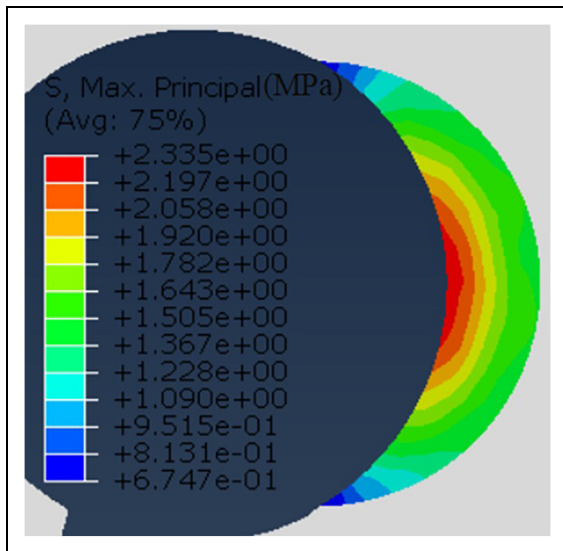


Figure 6. Control volume in polylactic acid (PLA)-3% tea model with notch radius 2 mm and notch inclination angle 75°.

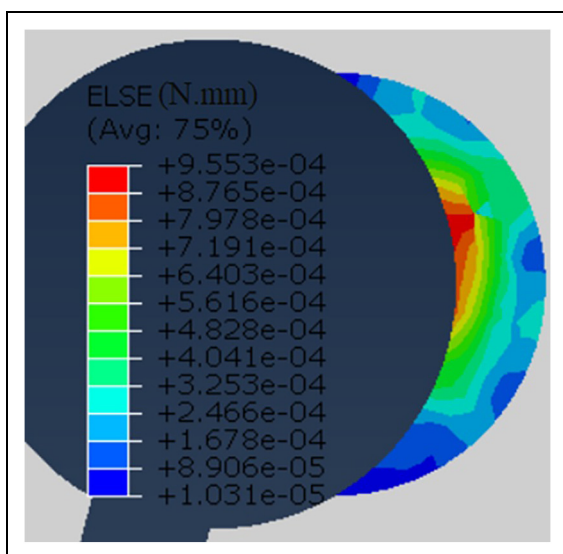


Figure 7. ELSE in PLA-3%Tea model with notch radius 2 mm and notch inclination angle 75°.

ELSE: strain energy magnitude in the element; PLA: polylactic acid.

Analysis

The morphology of the biocomposite was investigated using an SEM Tescan Mira3 instrument, operating at a voltage of 15 kV. In addition, the gold coating was applied to the specimens for microscopic imaging purposes.

The specimens underwent tensile and impact tests using a Santam STM-20 testing machine for tensile testing and a Santam SIT-20E machine for impact testing. Additionally, filament tensile tests and Poisson's ratio calculations were performed in collaboration with Dana Plastic Testing Company using a Speeco tensile testing machine. The tensile tests were conducted at a speed of 1 mm/min with a load cell of 50 kN.

Results and discussion

Microstructure morphology

Indeed, based on Figure 8(a), it is evident that the PLA-3% tea biocomposite demonstrates enhanced dispersion and uniformity of tea particles within the polymer matrix when compared to the PLA-5% tea biocomposite. This suggests a higher level of suitability between the tea particles and the base polymer in the PLA-3% tea composite. Furthermore, the agglomeration of particles in the PLA-5% tea biocomposite is significantly higher compared to the PLA-3% tea biocomposite. According to Figure 8(b), X-ray mapping analysis was performed based on carbon elements. In the Xmap test images, a significant accumulation of carbon elements is observed in the location of the tea waste particles, confirming the agglomeration of tea waste particles in the PLA-5% tea biocomposite. The presence of this agglomeration of tea waste particles in the PLA-5% tea biocomposite is expected to reduce the mechanical properties of this sample compared to the PLA-3% tea biocomposite. The reason for this behavior can be attributed to the weak bonding between the components of the tea waste agglomeration and the base polymer, as well as the presence of voids within this agglomeration, as evidenced in Figure 8(c).

Tensile test

The tensile test was conducted on filaments with a length of 10 cm and a diameter of 1.75 ± 0.1 mm. The data obtained from Table 3 and Figure 9 show that PLA-3% tea filament showed the highest tensile strength of 46 MPa. Furthermore, it should be noted that the PLA-5% tea filament possesses the lowest tensile strength, measuring 26 MPa. The difference in tensile strength between these two composites can be attributed to the agglomeration and poor dispersion of tea powder particles within the PLA matrix in the PLA-5% tea composite. As observed, the PLA-3% tea filament exhibits higher tensile strength even after undergoing two rounds of extrusion compared to the PLA filament.

As indicated in Table 4, the PLA-3% tea dog-bone specimen exhibits superior mechanical properties in terms of both strain and ultimate tensile strength when compared to the other specimens. With the increase of tea waste to 5% in the PLA-tea biocomposite, both the ultimate tensile strength and strain significantly decrease. This behavior is due to the insufficient composition of materials and particle density, which negatively affects the overall homogeneity and surface bonding in the composite. The stress-strain diagram for the dog-bone specimens is illustrated in Figure 10, whereas Table 4 presents the mechanical properties of the biocomposites. Furthermore, based on the results in Tables 3 and 4, it can be observed that standard specimens of PLA-tea waste biocomposites exhibit superior properties compared to the filaments of these compounds in relation to pure PLA.

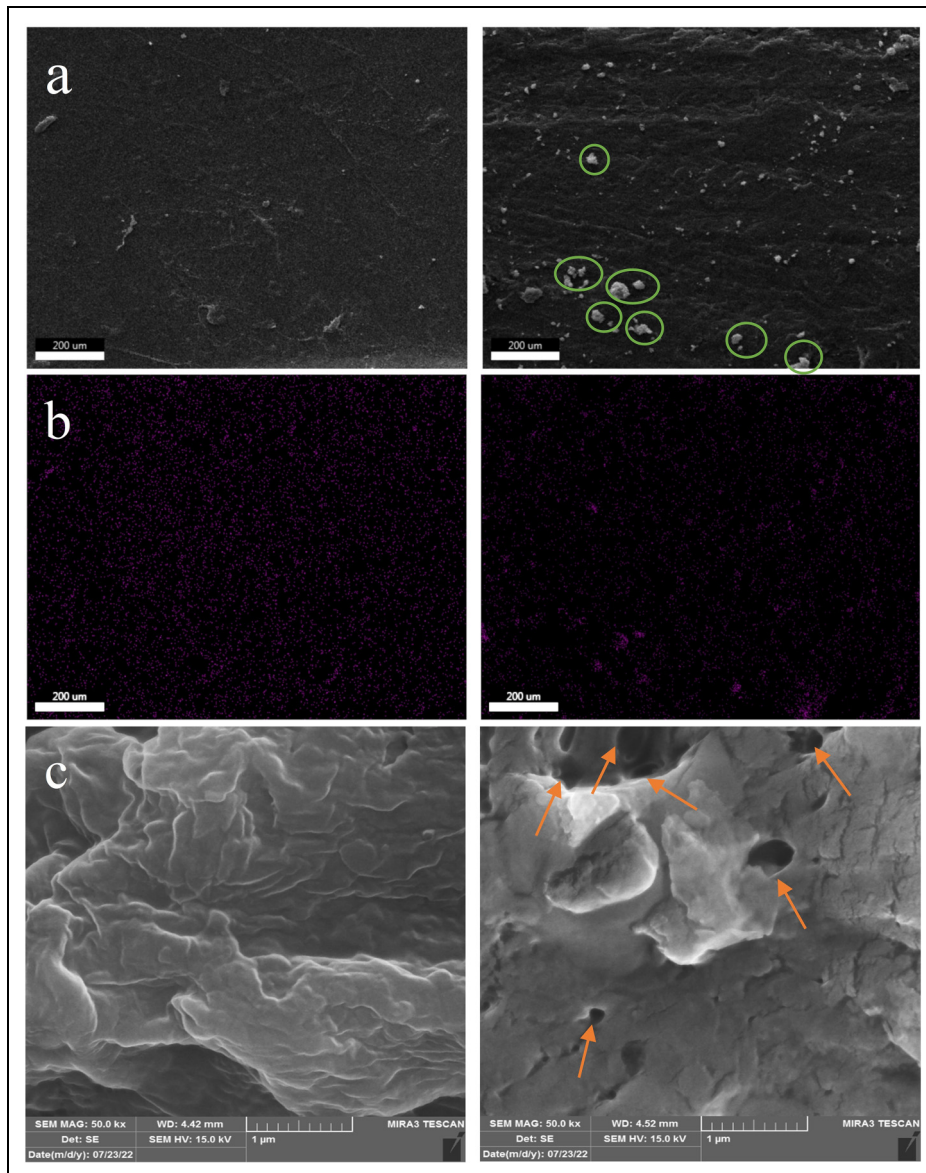


Figure 8. Morphological test on biocomposites PLA–3% tea (left) and PLA–5% tea (right): (a) SEM micrographs, (b) X-ray mapping of carbon element, and (c) SEM micrographs with high magnification.

PLA: polylactic acid; SEM: scanning electron microscopy.

Table 3. Tensile test data of filaments.

Specimen	σ_{ut} (MPa)	Strain
Polylactic acid (PLA)	37 ± 1.6	0.042 ± 0.002
PLA–3% tea	46 ± 3.9	0.035 ± 0.003
PLA–5% tea	26 ± 2.4	0.026 ± 0.001

This behavior is due to the presence of agglomerated tea waste particles in the samples of PLA–tea waste biocomposites. The presence of these agglomerates in the filaments of the biocomposites, due to their small filament diameter, can indeed have a significant effect on the reduction of the mechanical properties of the biocomposites. This issue is particularly noticeable in the tensile results of PLA–5%

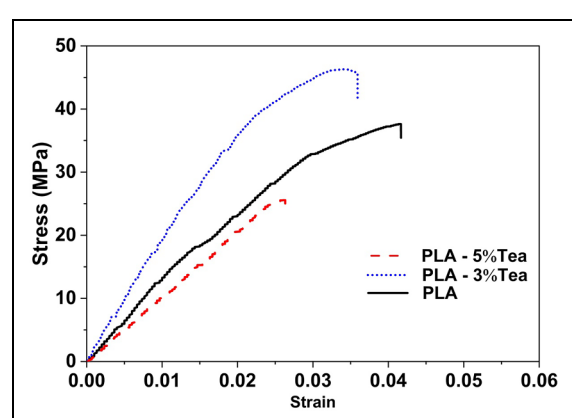
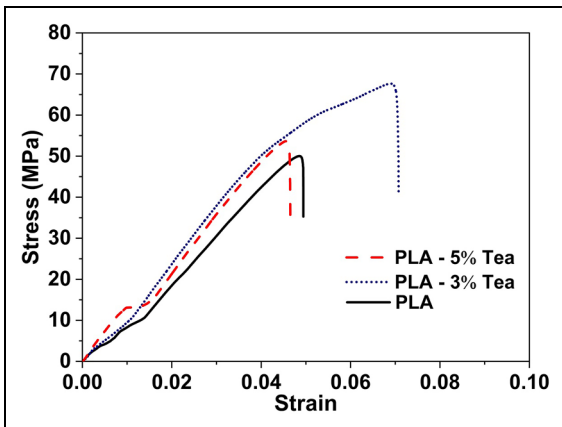
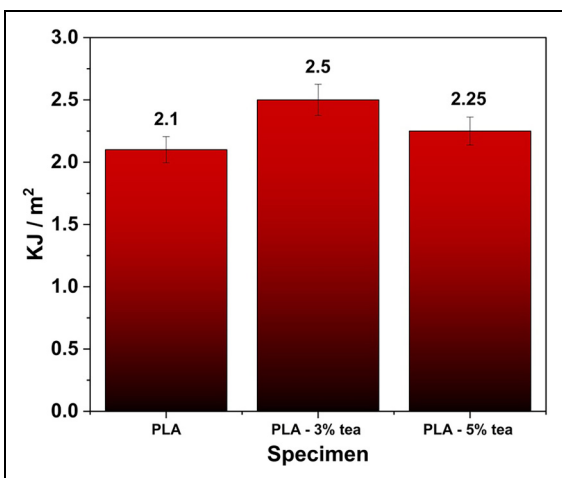


Figure 9. Stress–strain diagram of filaments.

Table 4. Mechanical properties of dog-bone specimens.

Specimen	σ_{ut} (MPa)	Strain	v	E (MPa)
Polylactic acid (PLA)	50 ± 3.3	0.049 ± 0.004	0.36	1142
PLA-3% tea	67 ± 5.7	0.07 ± 0.009	0.28	1259
PLA-5% tea	53 ± 5.4	0.047 ± 0.005	0.28	1351

**Figure 10.** Stress–strain diagram of dog-bone specimens.**Figure 11.** Fracture energy of specimens.

tea. The effect of the presence of these tea waste particles agglomerates in standard dog-bone specimens is less pronounced due to the larger size of the tensile specimens. Consequently, these biocomposites exhibit better tensile properties compared to PLA.

Impact Test

The results of the impact test are shown in Figure 11. The PLA-3% tea composite exhibits a fracture energy of 2.5 kJ/m^2 , while the PLA-5% tea biocomposite demonstrates a fracture energy of 2.25 kJ/m^2 . Therefore, the PLA-3% tea biocomposite is expected to be tougher and optimized. The biocomposite specimens after the impact test can be observed in Figure 12.

Numerical results of PLA–tea biocomposites with double keyhole notch

Based on the mechanical properties and the governing equations for the SED, the values of R_c , W_{cr} , and K_{lc} were calculated for the composite specimens, as shown in Table 5.

The F_{cr} for the PLA–tea biocomposites was estimated using numerical simulations in the ABAQUS® software, based on the mechanical properties provided in Tables 4 and 5. The results of these simulations are presented in Tables 6 and 7.

The F_{cr} for the PLA–tea biocomposite specimens can be observed in Tables 6 and 7. It can be seen that increasing the notch inclination angle and notch radius leads to a decrease in the F_{cr} value. For example, in Table 6, among the PLA-3% tea-75-0.5, PLA-3% tea-75-1, and PLA-3% tea-75-2 specimens, all with the same notch inclination angle of 75° , the PLA-3% tea-75-0.5 specimen with a

Table 5. R_c , W_{cr} , and K_{lc} values for polylactic acid (PLA)–tea composites.

Specimen	W_{cr} (N/mm ²)	K_{lc} (MPa· $\sqrt{\text{m}}$)	R_c (mm)
PLA-3% tea	1.783	3.45	0.73
PLA-5% tea	1.039	3.18	1.01

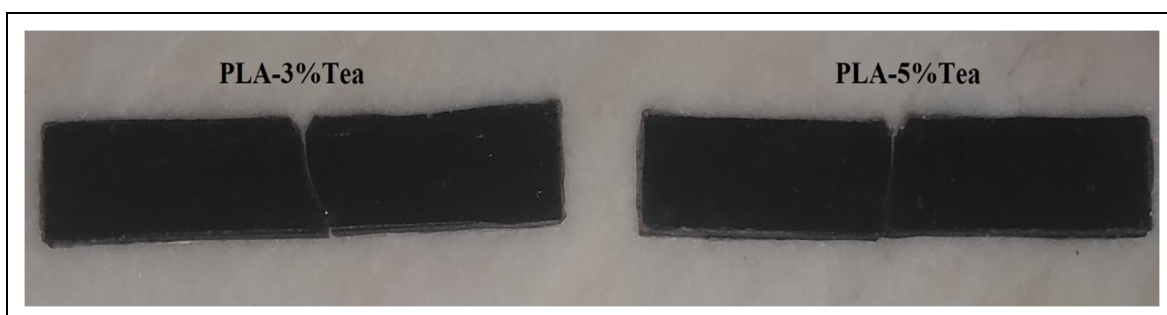
**Figure 12.** Biocomposite specimens after the impact test.

Table 6. Numerical test results of PLA-3% tea biocomposite with double keyhole notch specimens.

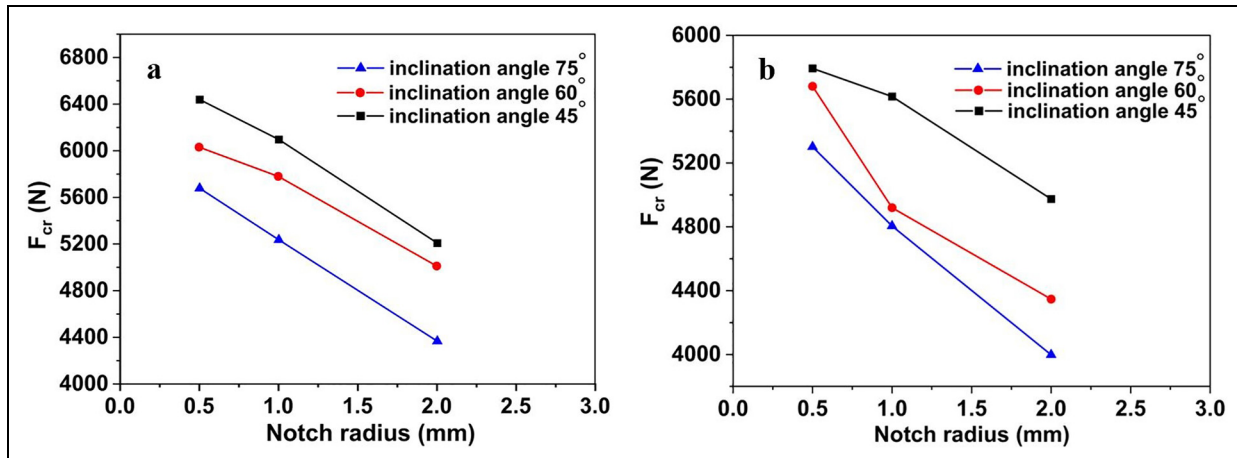
Specimen	β ($^{\circ}$)	ρ (mm)	φ ($^{\circ}$)	ELSE (N mm)	EVOL (mm 3)	W_{avg} (N/mm 2)	F_{cr} (N)
PLA-3% tea-45-0.5	45	0.5	50.11	0.008	18.65	0.00043	6439
PLA-3% tea-45-1	45	1	43.81	0.01	20.33	0.00049	6097
PLA-3% tea-45-2	45	2	46.87	0.015	22.4	0.00066	5208
PLA-3% tea-60-0.5	60	0.5	62.1	0.009	18.35	0.00049	6031
PLA-3% tea-60-1	60	1	62.4	0.011	20.17	0.00054	5780
PLA-3% tea-60-2	60	2	57.58	0.016	22.39	0.00071	5012
PLA-3% tea-75-0.5	75	0.5	63.32	0.01	18.3	0.00055	5678
PLA-3% tea-75-1	75	1	71.5	0.013	19.91	0.00065	5236
PLA-3% tea-75-2	75	2	75	0.021	22.38	0.00094	4367

ELSE: strain energy magnitude in the element; PLA: polylactic acid; EVOL: element volume.

Table 7. Numerical test results of PLA-5% tea biocomposite with double keyhole notch specimens.

Specimen	β ($^{\circ}$)	ρ (mm)	φ ($^{\circ}$)	ELSE (N mm)	EVOL (mm 3)	W_{avg} (N/mm 2)	F_{cr} (N)
PLA-5% tea-45-0.5	45	0.5	49.55	0.011	35.43	0.00031	5793
PLA-5% tea-45-1	45	1	47.16	0.013	39.08	0.00033	5617
PLA-5% tea-45-2	45	2	46.37	0.017	40.18	0.00042	4974
PLA-5% tea-60-0.5	60	0.5	62.91	0.012	37.62	0.00032	5681
PLA-5% tea-60-1	60	1	61.29	0.014	38.28	0.00043	4920
PLA-5% tea-60-2	60	2	58.88	0.022	40.21	0.00055	4347
PLA-5% tea-75-0.5	75	0.5	63.8	0.013	34.86	0.00037	5302
PLA-5% tea-75-1	75	1	72.88	0.017	37.63	0.00045	4805
PLA-5% tea-75-2	75	2	74.21	0.026	40.17	0.00065	3998

ELSE: strain energy magnitude in the element; PLA: polylactic acid; EVOL: element volume.

**Figure 13.** Effects of notch inclination angle and notch radius on F_{cr} : (a) polylactic acid (PLA)-3% tea and (b) PLA-5% tea.

notch radius of 0.5 mm has the highest F_{cr} , while the PLA-3% tea-75-2 specimen with a notch radius of 2 mm has the lowest F_{cr} . The decrease in F_{cr} in the PLA-3% tea-75-1 and PLA-3% tea-75-2 specimens in Table 6 can be attributed to the increase in the notch radius. As the notch radius increases, the cross-sectional area of the fracture decreases, resulting in a reduced load-carrying capacity of the specimen for fracture.

In the case of the PLA-5% tea-45-1, PLA-5% tea-60-1, and PLA-5% tea-75-1 specimens mentioned

in Table 7, all with a notch radius of 1 mm but differing in notch inclination angle, it can be observed that the PLA-5% tea-75-1 specimen with a notch inclination angle of 75° exhibits the lowest F_{cr} , while the PLA-5% tea-45-1 specimen with the notch inclination angle of 45° has the highest F_{cr} . The reason for this behavior is that with a decrease in the notch inclination angle, the stresses deviate from the direction of the applied load and spread across the notch surface. The F_{cr} behavior in PLA-3% tea and PLA-5% tea composite

specimens with a double keyhole notch can be observed with different notch inclination angles and notch radii in Figure 13.

Based on Figure 13, the PLA–3% tea and PLA–5% tea biocomposites exhibit similar behavior in simulated specimens with a double keyhole notch. In both composites, the F_{cr} decreases with an increase in the notch inclination angle and notch radius in the ABAQUS® simulation.

Conclusion

This study was conducted to enhance the mechanical properties of PLA through the incorporation of tea waste. A numerical investigation was also carried out on specimens featuring double keyhole notches. The results obtained from this study are presented below.

1. In the SEM images, it was observed that in the PLA–3% tea biocomposite, tea waste particles are uniformly and appropriately dispersed within the PLA matrix. However, in the PLA–5% tea biocomposite, the agglomeration of tea waste particles was observed. Therefore, it can be inferred that particle dispersion significantly affects the properties of PLA–tea biocomposites. The presence of agglomeration in PLA–5% tea biocomposites leads to a reduction in mechanical properties. The reason for this decrease in properties is the weak bonding between the components of the agglomeration and the presence of voids within them. Furthermore, it is possible that by implementing appropriate measures to prevent particle agglomeration, such as treating them, the properties of PLA–5% tea biocomposite may improve.
2. The results of the tensile and impact tests demonstrated that the incorporation of tea waste into PLA improved mechanical properties. The biocomposite PLA–3% tea exhibited the best performance, showcasing a 34% increase in tensile strength compared to pure PLA. The elongation also improved by 43% in the PLA–3% tea biocomposite compared to PLA. However, with an increase in the amount of added tea waste beyond 3% in PLA, both tensile strength and elongation noticeably decreased. In the tensile test, the filaments suitable for 3D printing also exhibited the highest mechanical properties within the biocomposite PLA–3% tea. Hence, the biocomposite PLA–3% tea is recommended as a substitute for pure PLA in the production of components using conventional methods and 3D printing across various industries.
3. In the conducted simulations on models featuring double keyhole notches, the biocomposite models of PLA–3% tea exhibited a higher F_{cr} value compared to the biocomposite models of PLA–5% tea in similar geometries. Additionally, it was observed that the F_{cr} decreases as the inclination angle of the notch and the radius of the notch increase.

Declaration of conflicting interests

The author(s) declared no potential conflicts of interest with respect to the research, authorship, and/or publication of this article.

Funding

The author(s) received no financial support for the research, authorship, and/or publication of this article.

ORCID iDs

Naser Kordani  <https://orcid.org/0000-0003-4464-9832>
Mahdi Bodaghi  <https://orcid.org/0000-0002-0707-944X>

References

1. Shanmugam V, Rajendran DJJ, Babu K, et al. The mechanical testing and performance analysis of polymer-fibre composites prepared through the additive manufacturing. *Polym Test* 2021; 93: 106925. doi:10.1016/j.polymertesting.2020.106925
2. Petousis M, Vidakis N, Mountakis N, et al. Multifunctional material extrusion 3D-printed antibacterial polylactic acid (PLA) with binary inclusions: the effect of cuprous oxide and cellulose nanofibers. *Fibers* 2022; 10: 52.
3. Zhang H, Zhang L, Liu Z, et al. Numerical analysis of hybrid (bonded/bolted) FRP composite joints: a review. *Compos Struct* 2021; 262: 113606. doi:10.1016/j.comstruct.2021.113606
4. Banea M, Rosioara M, Carbas R, et al. Multi-material adhesive joints for automotive industry. *Composites, Part B* 2018; 151: 71–77.
5. Ribeiro T, Campilho R, da Silva LF, et al. Damage analysis of composite–aluminium adhesively-bonded single-lap joints. *Compos Struct* 2016; 136: 25–33.
6. Katnam KB, Da Silva L and Young T. Bonded repair of composite aircraft structures: a review of scientific challenges and opportunities. *Prog Aerosp Sci* 2013; 61: 26–42.
7. Neto J, Campilho RD and Da Silva L. Parametric study of adhesive joints with composites. *Int J Adhes Adhes* 2012; 37: 96–101.
8. Guo J, Tsou C-H, Yu Y, et al. Conductivity and mechanical properties of carbon black-reinforced poly (lactic acid) (PLA/CB) composites. *Iran Polym J* 2021; 30: 1251–1262.
9. Zou D, Zheng X, Ye Y, et al. Effect of different amounts of bamboo charcoal on properties of biodegradable bamboo charcoal/polylactic acid composites. *Int J Biol Macromol* 2022; 216: 456–464.
10. Avci A, Eker AA, Bodur MS, et al. An experimental investigation on the thermal and mechanical characterization of boron/flax/PLA sustainable composite. *Proc Inst Mech Eng, Part L* 2022; 236: 2561–2573.
11. Jayswal A, Liu J, Harris G, et al. Thermo-mechanical properties of composite filaments for 3D printing of fabrics. *J Thermoplast Compos Mater* 2023; 36: 4800–4825.
12. Campilho RD, De Moura M and Domingues J. Modelling single and double-lap repairs on composite materials. *Compos Sci Technol* 2005; 65: 1948–1958.
13. Karthigeyan P, Raja MS, Hariharan R, et al. Performance evaluation of composite material for aircraft industries. *Mater Today Proc* 2017; 4: 3263–3269.
14. Parvez B, Kittur M, Badruddin IA, et al. Scientific advancements in composite materials for aircraft applications: a review. *Polymers (Basel)* 2022; 14: 5007.

15. Shelley J, LeClaire R and Nichols J. Metal-matrix composites for liquid rocket engines. *Jom* 2001; 53: 18–21.
16. Gross D and Seelig T. *Fracture mechanics: with an introduction to micromechanics*. 3rd ed. Cham: Springer Publishing, 2017.
17. Msekha MA, Cuong N, Zi G, et al. Fracture properties prediction of clay/epoxy nanocomposites with interphase zones using a phase field model. *Eng Fract Mech* 2018; 188: 287–299.
18. Wang E, Zhou W and Shen G. Three-dimensional finite element analysis of crack-tip fields of clamped single-edge tension specimens—part I: crack-tip stress fields. *Eng Fract Mech* 2014; 116: 122–143.
19. Xiao J, Wang G, Wang Y, et al. Two-parameter fracture prediction for cracked plates under bending. *Eng Fract Mech* 2021; 255: 107974.
20. Cui P and Guo W. Higher order J-Tz-AT solution for three-dimensional crack border fields in power-law hardening solids. *Eng Fract Mech* 2019; 222: 106736.
21. Lazzarin P and Zambardi R. A finite-volume-energy based approach to predict the static and fatigue behavior of components with sharp V-shaped notches. *Int J Fract* 2001; 112: 275–298.
22. Lazzarin P and Berto F. Some expressions for the strain energy in a finite volume surrounding the root of blunt V-notches. *Int J Fract* 2005; 135: 161–185.
23. Weng L, Huang L, Taheri A, et al. Rockburst characteristics and numerical simulation based on a strain energy density index: a case study of a roadway in Linglong gold mine, China. *Tunn Undergr Space Technol* 2017; 69: 223–232.
24. Fajdiga G, Ren Z and Kramar J. Comparison of virtual crack extension and strain energy density methods applied to contact surface crack growth. *Eng Fract Mech* 2007; 74: 2721–2734.
25. Sih GC. *A special theory of crack propagation. Mechanics of fracture initiation and propagation: surface and volume energy density applied as failure criterion*. Dordrecht: Springer Netherlands, 1991, p. 1–22.
26. Yishu Z. A strain energy criterion for mixed mode crack propagation. *Eng Fract Mech* 1987; 26: 533–539.
27. Soltaninezhad S, Salavati H and Goharrizi AS. Ductile fracture assessment of high-density polyethylene (HDPE-PE100) weakened by an inclined double keyhole notch. *Theor Appl Fract Mech* 2019; 104: 102349.
28. Berto F, Lazzarin P, Gómez F, et al. Fracture assessment of U-notches under mixed mode loading: two procedures based on the ‘equivalent local mode I’ concept. *Int J Fract* 2007; 148: 415–433.
29. Yosibash Z, Bussiba A and Gilad I. Failure criteria for brittle elastic materials. *Int J Fract* 2004; 125: 307–333.
30. Lazzarin P and Filippi S. A generalized stress intensity factor to be applied to rounded V-shaped notches. *Int J Solids Struct* 2006; 43: 2461–2478.
31. Salavati H, Alizadeh Y and Ayatollahi MR. Fracture assessment of inclined double keyhole notches in isostatic graphite. *Phys Mesomech* 2018; 21: 110–116.

Appendix

Notation

PLA	polylactic acid
E	Young's modulus
ν	Poisson's ratio
R_C	control radius
σ_{00}	stresses at a distance r from the local frame origin
σ_{ut}	ultimate tensile strength
K_{Ic}	fracture toughness
F_{cr}	critical fracture load
F_{ap}	applied load
SED	strain energy density
W_{cr}	critical SED
W_{avg}	averaged SED over the related control volume
ELSE	strain energy magnitude in the element
EVOL	element volume